I&EC research
Industrial & Engineering Chemistry Research

pubs.acs.org/IECR
Article

Study of the Solvent-Free Process of Enzymatic Synthesis of Pentyl Esters in a Packed Bed Reactor (PBR) Using the Lipozyme435 Heterogeneous Biocatalyst

Beatriz Lorenzo,* Juan Ortega,* ÁlvaroGonzález Garcinuño, and EvaMartín-del Valle

Cite This: https://doi.org/10.1021/acs.iecr.5c02780
Read Online

ABSTRACT: This article describes a solvent-free enzymatic esterification process for the production of pentyl acetate or pentyl propanoate from pentanol and the corresponding acetic or propanoic acids. Both reactions were carried out in a continuous packed bed reactor (PBR) using the immobilized lipase Lipozyme435 as the catalyst. The effect of several variables was analyzed to determine the most suitable conditions: temperature, proportion of reactants, and flow rate of the products in the reactor. High conversions of the acid substrate (above 80%) were obtained at all working temperatures for an alcohol-to-acid molar ratio of 2 and flow rates up 1 mL/min, demonstrating the technical feasibility of the reactor configuration for this type of synthesis. However, it was observed that the enzyme lost activity due to the synergistic effect of high temperatures (>70 °C) and an equimolar alcohol-to-acid ratio, exhibiting a behavior similar to that observed when using a batch stirring reactor (BSTR). In contrast to observations in a batch stirring reactor (BSTR) under the same conditions, the synthesis process in the PBR at 70 and 80 °C with a 2:1 alcohol-to-acid molar ratio showed no signs of enzymatic deactivation. This behavior suggests that scaling up the process for continuous industrial production is more advantageous than using small-scale batch processes. The economic indicators of the biocatalytic processes calculated here also indicated that PBR reactors are preferable for large-scale production.

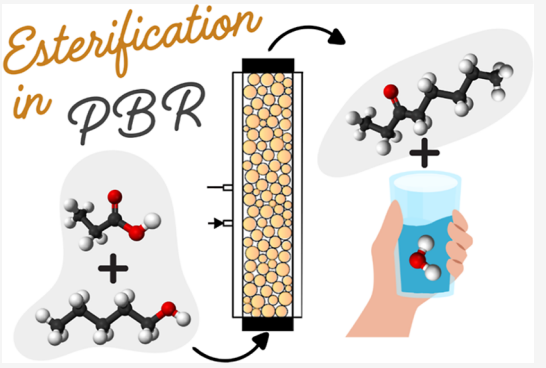

1. INTRODUCTION

Biocatalytic processes have great potential for industrial applications. However, their use in industrial sectors is limited by the nonviability of the process, as determined by certain economic metrics such as the achievable concentration of the product in the reaction medium, the yield (calculated as the percentage ratio of the mass of product to achievable mass of the substrate), the volumetric yield (defined as the product mass/time/reactor volume), and the catalyst yield (defined as product mass/catalyst mass).[1,2] These and other limitations can be overcome by certain bioprocess intensification strategies, as proposed by several authors.[3,4] Some are (i) using enzymes immobilized on solid supports,[5] (ii) using solvent-free reactive processes,[4] and (iii) using continuous flow reactors.[5,6] However, in order to make the processes industrially scalable, most of the current research on enzymatic esterification processes focuses on using batch reactors that work with low concentrations of reactants in organic solvents. Therefore, the synthesis processes proposed in this work will be approached with the aim of evaluating the aforementioned strategies using a continuous flow reactor, as indicated in (iii).

The current literature contains few publications on immobilized enzymatic esterification processes involving reactions of short-chain carboxylic acids with alcohols in continuous-flow-reactors.[7−22] Moreover, only three of these publications[14,18,19] provide information on reactive systems under solvent-free conditions. Of these, only one[19] uses acetic or propanoic acid as an acyl donor without considering the acidic effect on enzyme stability.

In this work, the solvent-free heterogeneous enzymatic esterification process was studied by reacting pentan-1-ol with acetic acid and propanoic acid to produce the corresponding esters of pentyl acetate and propanoate. These esters have a wide range of applications as additives in the flavor and fragrance industry, in the manufacture of adhesives and plastics, and as solvents in the chemical and pharmaceutical industries. The extraction of penicillin is a notable and special case.[23,24] Previous investigations on the synthesis of pentyl acetate in a batch reactor without using solvents[25] showed promising results. Here, we analyzed and compared the results obtained using a batch stirrer tank reactor (BSTR) with those obtained using a

Received: July 8, 2025
Revised: July 14, 2025
Accepted: July 15, 2025

https://doi.org/10.1021/acs.iecr.5c02780
Ind. Eng. Chem. Res. XXXX, XXX, XXX−XXX

continuous flow-packed bed reactor (PBR), assessing the effects of different operating conditions by modifying the following variables: temperature, molar ratio of reagents, and flow rate through the reactor. Thus, the heterogeneous enzymatic esterification process was explored from a broad research perspective by simultaneously considering the three aforementioned strategies (i)−(iii) to improve the synthesis processes. The results of the synthesis of the two pentyl esters in the PBR were compared, from a technical and economic standpoint, with those obtained in a BSTR[25] reactor equipped with a U-shaped paddle stirrer and operating with biocatalyst particles in suspension. The aim of this comparison was to determine the optimal conditions for producing the aforementioned pentyl esters.

2. EXPERIMENTAL SECTION

2.1. Materials and Equipment. The reagents used in the esterification reactions were pentan-1-ol, acetic acid, and propanoic acid, supplied by Merck and of the highest commercial quality. Due to the presence of water as the final product of the reaction, the initial moisture content of the compounds was determined by Karl Fischer coulometric titration (Mettler, C-20). In addition, before use, the substances were degassed by ultrasound and stored for several days in the dark on a Fluka 3 Å molecular sieve. Final quality was determined by gas chromatography (Varian-450 GC) equipped with a flame ionization detector and a standard HP-5 capillary column, programmed with an initial temperature of 80 °C, a ramp of 10 °C/min, and a stabilization time of 10 min at 120 °C. Helium was used as a carrier gas at a flow of 2 mL/min. The purity values were slightly better than those stated by the manufacturer. After these operations, the density (Anton-Paar, 60/602) and the refractive index (Zuzi, 320) were measured at 298.15 K and atmospheric pressure, giving values in agreement with those of literature,[26−29] see Table S1.

Blue dextran (Merck) and sodium azide (Panreac), of purity quality >99%, were used as pulse tracers in the residence time distribution (RTD) experiments. In the esterification process, the enzyme Lipozyme435 supplied by Novonesis (formerly Novozymes) was used, an enzymatic catalyst obtained by immobilization of *Candida antarctica* lipase B on the macroporous poly(methyl methacrylate) (PMMA, main component of the particles) Lewatit VP OC 1600 resin.[30] The manufacturer specifies that the enzyme has an activity of 9000 PLU/g.

2.2. Packed Bed Reactor Configuration. The continuous reaction process was carried out in a PBR consisting of a glass column (Ø = 1.6 cm and L = 14 cm), filled with 6 g (≈2 cm^3) of biocatalyst. The reactive process in the PBR was quasi-isothermal at ($t \pm 0.1$) °C, achieved by supplying a constant water flow rate of 12 L min^{-1} using a thermostatically controlled bath (P-Selecta, TFT-10), through a concentric jacket with the main body of the reactor, as shown in Figure 1. A Heidolph peristaltic pump (model 5201 C8) was used to flow the reagents through the PBR.

One of the most important aspects of modeling the reactive process in the PBR was the characterization of the support used for lipase immobilization and the biocatalyst bed in the reactor. This was done by determining two relevant parameters: the particle size distribution (PSD) and porosity ε_p, of the support and the porosity of the bed ε_b. The procedure is described below.

a To determine the PSD, which characterizes the enzyme on a dry basis, a Malvern Mastersizer 2000 (Malvern, Instruments, UK) was used. The chamber was filled with ∼0.7 g, using distilled water as the liquid medium and stirring the solution at 850 rpm to ensure a turbulent flow inside the chamber. The laser provided values that estimated the PSD for a mean particle diameter, which after several experiments was of 593 μm (∼0.6 nm), as shown in Figure 2. This value is slightly higher than those found in other works.[30,31] The uniformity was 0.3 with a span of 0.976, indicating adequate monodispersity.

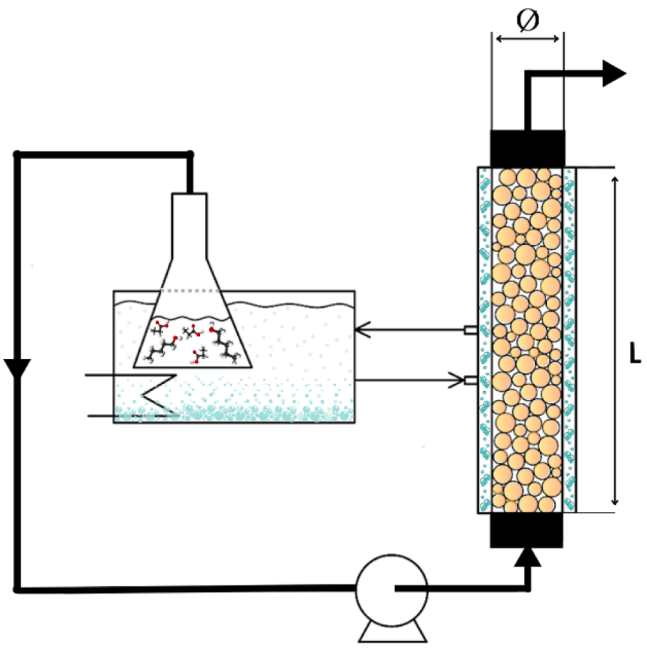

Figure 1. PBR setup.

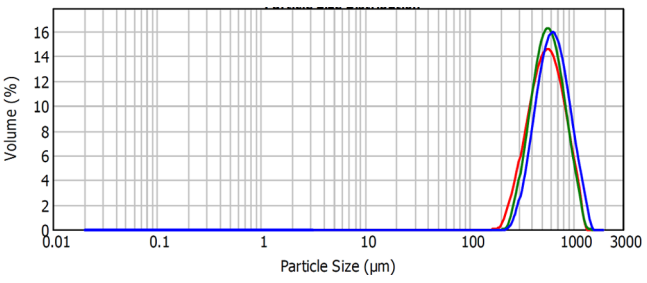

Figure 2. PSD of the Lipozyme435 catalyst (wet basis, Mastersizer 2000). Colors represent each experiment.

b The porosity of the particles ε_p was determined using two different methods.

b.1 Using the BET method for the dry material, which is based on the adsorption of nitrogen (N_2), as an adsorbate, at low temperature to determine the area of a solid. The samples were predegassed at 110 °C for 2 h under a stream of dry N_2 in a Micromeritics FlowPrep 060 system. The adsorption−desorption isotherms were calculated by maintaining the temperature of the Dewar vessel at −196 °C with liquid N_2, a temperature at which thermal degradation was not expected. The surface area and pore volume were calculated using a Micromeritics Gemini VII 2390t, and the BET analysis revealed a surface area of 64.2 m^2 g^{-1} with an average pore size of 11.6 nm. The total specific pore volume was estimated from the isotherm to

https://doi.org/10.1021/acs.iecr.5c02780
Ind. Eng. Chem. Res. XXXX, XXX, XXX−XXX

be 0.19 $cm^3\ g^{-1}$. Considering the actual density (1170 kg/m^3) of PMMA, the porosity of dry particles was $\varepsilon_p = 0.22$.

b.2 On the other hand, the porosity of the wet particles of the biocatalyst and the bed was determined by studying the nonideal flow of two tracers, blue dextran and sodium azide, through the reactor bed.[32] The justification for using these tracers is that the blue dextran has a high molecular weight (>2000 kDa) and molecular size (≈80 nm),[33] which prevents it from passing through the particleś pores (11.6 nm), diffusing only in the extra-particle space. Conversely, sodium azide has a low molecular weight (65 Da) and diffuses in the outer and inner spaces of the particles, exhibiting a delayed RTD. With the combination of both RTD results, the porosities corresponding to the intraparticle and extra-particle are determined.[34] For both experiments, the water flow through the PBR reactor was kept constant at 1.2 mL·min^{-1}. Blue dextran (1 mg·mL^{-1}) and sodium azide (0.1 mg·mL^{-1}) were administered separately in 8.4 mL pulses. Aliquots of 1 mL were collected at the reactor outlet, and the concentrations were obtained by spectrophotometry (Shimadzu UV-1800) at 618 nm for blue dextran and at 236 nm for sodium azide. The graphical results of RTD for both tracers are shown in Figure A1, see Appendix A1. The calculated biocatalyst porosity was $\varepsilon_p = 0.40$, and the corresponding porosity was $\varepsilon_b = 0.64$. This result may raise doubts because of the difference with the value obtained by the BET method. However, it is important to take into account that the particles were wet and swollen by water, as highlighted in a recent study.[35] The latter value was used in the calculations, as the reactions studied in this work occur in the liquid phase.

2.3. Description of the Esterification Procedure. The esterification reactions for the two pentyl esters were carried out in a PBR reactor, as described below. To determine the best working conditions, the experiments were performed by setting different values for the following variables: (i) temperature: t/°C = 40, 50, 60, 70, and 80; (ii) total flow rate through the reactor: $\dot{Q}$ = 0.7, 1, 2, and 3 mL/min, corresponding to mean residence times of 26, 18, 9, and 6 min, respectively, depending on the reactor volume and bed porosity; and (iii) ratio of reagents: $C_{0,alcohol}/C_{0,acid}$ = 1 and 2 when the reagent was propanoic acid, and $C_{0,alcohol}/C_{0,acid}$ = 2 when acetic acid reacted. In the latter case, the ratio $C_{0,alcohol}/C_{0,acid}$ = 1 was not considered, since a previous work[25] showed that systems with a higher acid concentration resulted in a loss of enzymatic activity. This is because a possible acid inhibition prevents the substrate−enzyme contact, hindering the biocatalysts action in the reaction. The condition of $C_{0,alcohol}/C_{0,acid}$ = 1 corresponds to equimolar concentrations of the two reagents; i.e., $C_{0,acid} = C_{0,alcohol}$ = 5.3 mol/L. When $C_{0,alcohol}/C_{0,acid}$ = 2, the concentrations of alcohol and acid were $C_{0,alcohol}$ = 6.6 mol/L and $C_{0,acid}$ = 3.3 mol/L, respectively, for the case of propanoic acid, and $C_{0,alcohol}$ = 7.2 mol/L and $C_{0,acid}$ = 3.6 mol/L for the case of acetic acid.

The sequence of the procedure for each experiment is as follows: Once the working temperature t/°C was set, the reaction began with the pumping of the reagent mixture and setting the conditions (ii) and (iii) described above. In all cases, the duration of each reaction cycle was set to approximately 3 h. The first sample of the effluent of the reactor was taken after 10 min and then repeatedly every 30 min. The steady state was reached approximately 30 min after starting. The samples were analyzed using acid−base titration of the unreacted carboxylic acid with a standard NaOH solution and phenolphthalein (1% in ethanol) as an indicator. The estimated error in calculating the sample concentration was less than 5%. The results were verified by GC and showed little differences from the stated procedure. Before each experiment, it was also checked that the hydrolysis of the ester did not affect the titration results. The conversion percentage was calculated using the simple following relationship: $100(C_{0,acid} - C_{i,acid})/C_{0,acid}$.

3. RESULTS AND DISCUSSION

The conversions achieved in the PBR for the different operating conditions mentioned in the previous section are shown in Figure 3. When $C_{0,alcohol}/C_{0,acid}$ = 2 (i.e., with a double excess of alcohol), the results of synthesizing both esters were similar. The conversion was higher at higher temperatures but decreased with increased flow rate $\dot{Q}$; see Figures 3a,c and S1. The evolution of the conversion seems logical and suggests the following: (a) the enzyme deactivation was almost nonexistent when $C_{0,alcohol}/C_{0,acid}$ = 2 and did not depend on the working temperature and (b) the increase in flow rate was inversely proportional to the degree of conversion as the reagent/catalyst contact decreases.

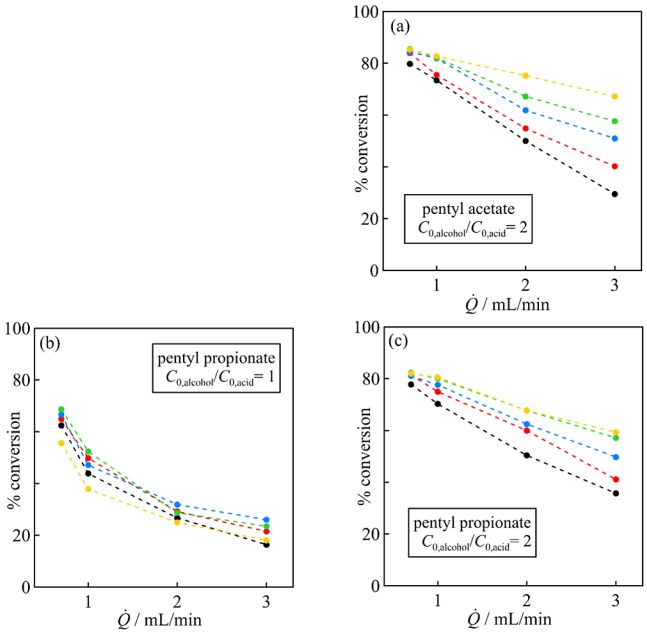

Figure 3. Conversion achieved in the PBR reactor as a function of different values of the following variables: temperature, flow rates, and alcohol/acid molar ratio. (a) Synthesis of pentyl acetate with $C_{0,alcohol}/C_{0,acid}$ = 2; (b) synthesis of pentyl propanoate with $C_{0,alcohol}/C_{0,acid}$ = 1; (c) synthesis of pentyl propanoate with $C_{0,alcohol}/C_{0,acid}$ = 2. t/°C = (●) 40, (●—red) 50, (●—blue) 60, (●—green) 70, and (●—yellow) 80.

The results with the ratio $C_{0,alcohol}/C_{0,acid}$ = 1, i.e., an equimolar solution, showed a different trend, Figure 3b. At first glance, the conversion percentages were lower than in previous cases, but in addition, the dependence of the conversion on the temperature was irregular. Figures S1a,b shows that at low flow rates (0.7−1 mL/min), the conversion increases with temperature up 70 °C and subsequently decreases up to 80 °C. At higher flow rates (2−3 mL/min), the conversion increases up 60 °C and then gradually decreases; see Figures S1c,d. This indicates that the

https://doi.org/10.1021/acs.iecr.5c02780
Ind. Eng. Chem. Res. XXXX, XXX, XXX−XXX

enzymatic deactivation occurs above 70 °C for the equimolar ratio of reagents concentration, as discussed in the introduction. However, in addition to the above, the acid inhibition of the biocatalyst, which prevents catalyzing the reaction, causing the conversion to decrease, cannot be ruled out.[37]

In summary, the synthesis of pentyl esters in a PBR exhibited a good operating stability considering for the experiences of this work an operational time of 3 h, see Figure S2. This suggests that such a reactor configuration could be useful for larger scale applications. Based on the experience of previous works,[25] in which the enzyme was reused for up to ten successive 8 h cycles without deactivation, it was expected that the enzyme would also remain stable in the PBR for over 8 h of operation.

The information obtained makes it possible to compare the results of the esterification process for producing pentyl esters in two types of reactors, PBR and BSTR, operating under the same conditions. The kinetics in a BSTR reactor, previously described,[25] produced the data shown in Figures S3 and S4. Figure 4 compares the degree of conversion results as a function

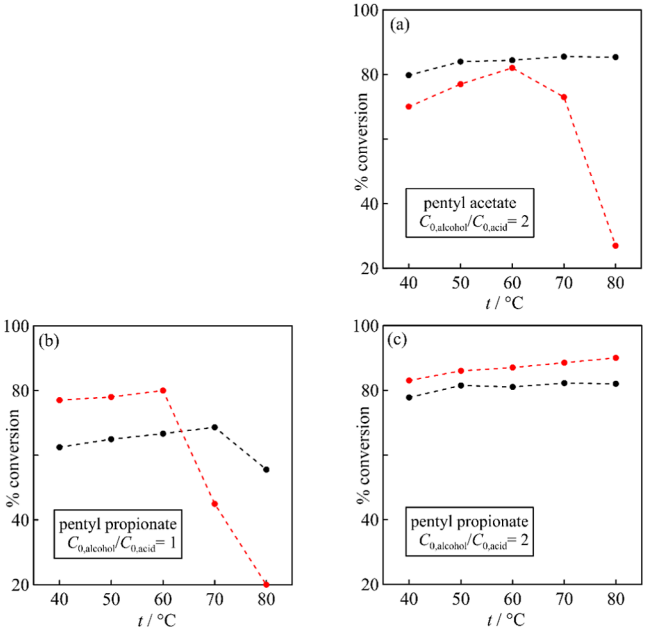

Figure 4. Conversion achieved in the BSTR (red) and PBR (black) reactors as a function of temperature considering the synthesis of (a) pentyl acetate with $C_{0,alcohol}/C_{0,acid}$ = 2; (b) pentyl propanoate with $C_{0,alcohol}/C_{0,acid}$ = 1; and (c) pentyl propanoate with $C_{0,alcohol}/C_{0,acid}$ = 2. In the BSTR, the reaction proceeded at a weight ratio of $w_{catalyst}/w_{acid}$ = 0.1 for 5 h. In the PBR, the reaction proceeded at $\dot{Q}$ = 0.7 mL/min, see Table S2.

of the temperature in both reactors. These figures reveal several interesting facts:

(1) The enzyme shows a higher thermal stability in the PBR.
(2) In the synthesis of pentyl acetate, the figures show that, using a ratio $C_{0,alcohol}/C_{0,acid}$ = 2 in the PBR, the temperature hardly affects the deactivation of the enzyme, but it does occur in the BSTR from 60 °C, see Figure 4a. However, in the synthesis of pentyl propanoate carried out in the PBR with $C_{0,alcohol}/C_{0,acid}$ = 1, a slight loss of enzymatic activity is observed from 70 °C, see Figure 4b, whereas in the BSTR, a strong deactivation of the enzyme occurs from 60 °C. This fact, in addition to other factors that will discuss, can also be explained by the inhibitory action of the enzyme, as indicated above. Other researchers have reported this for different enzymes.[36−42] Some authors[36,39] suggested that the lower deactivation of the enzyme in the PBR is due to the constant flow of reagent, which prevents both the heat energy accumulation and the local temperature increase. Others[42] explain this by considering a combination of thermo-mechanical effect on the catalyst in the batch reactor due to the shear forces of the stirrer (this is a function of the number of rpm) and the inhibition by the product. Figure 4c shows that, in the case of synthesis of pentyl propanoate with the initial concentration ratio of $C_{0,alcohol}/C_{0,acid}$ = 2, the degree of conversion was quite similar in both reactors, although with a slight increase with temperature, as previously mentioned.

In addition, the information obtained allows the calculation of certain economic metrics applicable to the scaling-up of biocatalytic processes. These metrics consider each reactor, as described by Tufvesson et al.,[1] see Table S2, in order to estimate the operating window in which the process could be feasible. Threshold values for specific chemicals were used for screening (conversion >80% and $kg_{ester} \cdot kg_{biocatalyst}^{-1}$ > 100). This initial screening reduced the number of reaction experiments from 84 to 31, see Figure 5a. With this information, we can make other

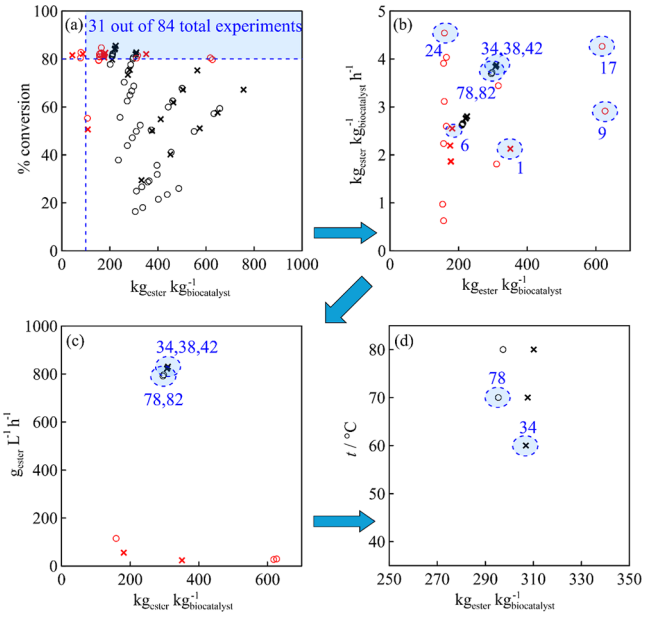

Figure 5. Benchmarking to optimize the scaling-up of reaction conditions according to different metrics[1,2] and considering the reactor type: BSTR (red) and PBR (black). Symbols indicate the ester: × pentyl acetate and ◯ pentyl propanoate. The blue numbers refer to the codes established in Table S2, which considers the experimental conditions. (a) % conversion vs biocatalyst yield, (b) biocatalyst productivity vs biocatalyst yield, (c) volumetric productivity vs biocatalyst yield, and (d) operating temperature vs biocatalyst yield.

general considerations, taking into account the different conditions used in this work, which we briefly discuss. For BSTR reactors, an operating window can be established with a catalyst loading of less than 10 wt %, Figure S5, in the reaction medium and temperatures within the range of 40−70 °C, except for the synthesis of pentyl propanoate with a ratio of $C_{0,alcohol}/C_{0,acid}$ = 2, at t = 40−80 °C. For PBR, see Figure S6, the operating window for the same ratio corresponded to flow rates of up to 1

https://doi.org/10.1021/acs.iecr.5c02780
Ind. Eng. Chem. Res. XXXX, XXX, XXX−XXX

mL/min and temperatures between 50 and 80 °C. PBR systems with $C_{0,alcohol}/C_{0,acid}$ = 1 are not suitable for scale-up because none meets the specified criteria.

Other productivity-related metrics were evaluated to determine the optimal conditions for synthesizing each ester. Figure 5a shows the conversion vs the biocatalyst yield. Figure 5b shows the biocatalyst productivity, $kg_{ester}{\cdot}kg_{biocatalyst}^{-1}{\cdot}h^{-1}$ vs biocatalyst yield, $kg_{ester}{\cdot}kg_{biocatalyst}^{-1}$. Nondominated points were selected for each reaction system, including the closely related ones, reducing the number of reaction conditions according to different metrics to 10. The production capacity was analyzed by comparing the volumetric productivity, $g_{ester}{\cdot}L^{-1}{\cdot}h^{-1}$, see Figure 5c. This revealed that continuous flow was 7−35 times more productive than batch systems. Similar results were obtained for all calculated metrics for these PBR systems, so a final selection was made based on the operating temperature, Figure 5d. The optimal conditions for PBR were a flow rate of 1 $mL{\cdot}min^{-1}$, which correspond to a residence time of 18 min, a $C_{0,alcohol}/C_{0,acid}$ = 2 and a temperature of 60 °C, for pentyl acetate synthesis and 70 °C for pentyl propanoate synthesis.

4. MODELING THE ESTERIFICATION PROCESS IN A PBR

According to the RTD results in Appendix A, the axial dispersion model[43] is an effective alternative for modeling the PBR, as it represents a piston flow with a minimal axial dispersion. When the radial dispersion is neglected, the differential equation describing the variation of the concentration with time and length of PBR the axial dispersion model is described by the following equation:

$$D_{ax}\frac{\partial^2 C}{\partial z^2} - \frac{u}{\varepsilon_b}\frac{\partial C}{\partial z} + r = 0 \quad (1)$$

The values in Table B1 indicate that the effects of external mass transfer are not significant in the PBR; however, the internal mass transfer must be considered, resulting in the following equation:

$$D_{ax}\frac{\partial^2 C}{\partial z^2} - \frac{u}{\varepsilon_b}\frac{\partial C}{\partial z} + \eta_I r_{obs} = 0 \quad (2)$$

On the other hand, the reaction rate r_{obs} is modeled by the so-called Bi−Bi Ping Pong kinetic mechanism in the case of biocatalytic reactions. This model produced good results in the synthesis of pentyl acetate carried out in a BSTR.[25] Therefore, its application in this work is also discussed in the Supporting Information, where it was used as a method to calculate the reaction rate for PBR modeling, complementing the dispersion model.

Since the experimental value D_{ax} in Table A1 was determined for a single value of flow and temperature, for using in eq 2, the value of D_{ax} is calculated using the method of Chung and Wen,[44] expressed by

$$\frac{\varepsilon_b u d_p}{D_{ax}} = 0.20 + 0.011Re^{0.48} \quad (3)$$

The resolution of this equation is formulated as a boundary problem applying on it the conditions established by Danckwerts,[45] where

$$C_{acid}\langle z = 0\rangle = C_{0,acid}\frac{\partial C_{ac}}{\partial z}\langle z = L\rangle = 0 \quad (4)$$

This was solved numerically for each of the conditions imposed on the reaction using a widely used Runge−Kutta (RK) method, the fourth-order Lobatto IIIA type.[46] The results of the RK-Lobatto IIIA binomial implementation are listed in Figure 6a−c. Depending on the temperature range, the comments on

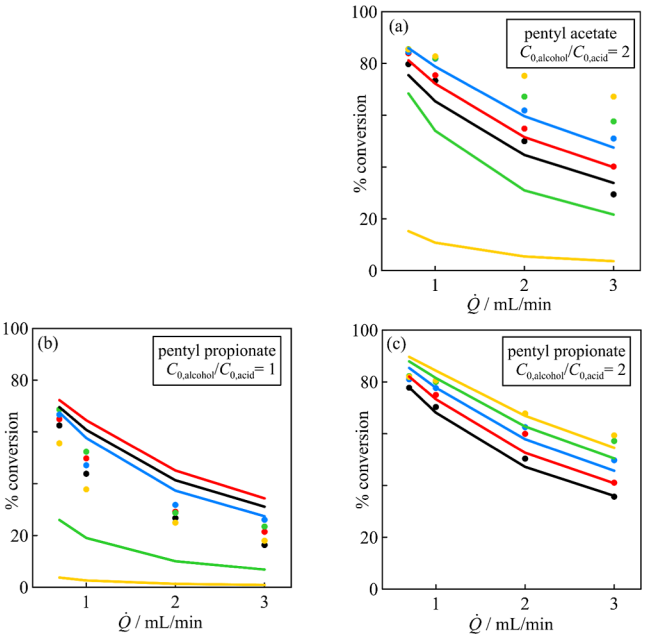

Figure 6. Modeling of the kinetics (solid-lines) in a PBR according to eqs 2−4 for the synthesis of (a) pentyl acetate at $C_{0,alcohol}/C_{0,acid}$ = 2; (b) pentyl propanoate at $C_{0,alcohol}/C_{0,acid}$ = 1; and (c) pentyl propanoate at $C_{0,alcohol}/C_{0,acid}$ = 2, as a function of flow rate and temperature. Symbols correspond to experimental values at different temperatures: (●) 40 °C (●—red) 50 °C, (●—blue) 60 °C, (●—green) 70 °C, and (●—yellow) 80 °C.

the modeling of the kinetics in the PBR were set according to two different scenarios:

(i) 40−60 °C: In this range, up to 60 °C, the conversion found by the model is very similar to the experimental one and independent of the flow. The largest deviation corresponds to the synthesis of pentyl propanoate with a ratio of $C_{0,alcohol}/C_{0,acid}$ = 1, as the model overestimates the achievable conversion.

(ii) 70−80 °C: In this temperature range, the model underestimates the conversions for the synthesis of pentyl acetate when $C_{0,alcohol}/C_{0,acid}$ = 2 and that of pentyl propanoate for $C_{0,alcohol}/C_{0,acid}$ = 1. The reason for this is that the calculation of the reaction rate is based on batch experiments, and for these systems, a strong enzyme deactivation is observed at these temperatures, whereas the thermal stability of the enzyme, and thus the reaction rate, is much higher in the PBR, as discussed in Section 3. On the other hand, for the synthesis of pentyl propanoate with $C_{0,alcohol}/C_{0,acid}$ = 2, Figure 5c, the model represents well the experimental conversion since for this system, the enzyme stability in the batch reactor was found to be in agreement with that shown for the PBR.

5. CONCLUSIONS

In this work, we examined the feasibility of carrying out the continuous production of pentyl acetate and pentyl propanoate

https://doi.org/10.1021/acs.iecr.5c02780
Ind. Eng. Chem. Res. XXXX, XXX, XXX−XXX

from their respective carboxylic acids and pentanol in solvent-free conditions using a PBR with a biocatalyst Lypozyme435. We found no similar proposals in the literature regarding configuration or working conditions of the reactor for synthesizing short-chain esters, as most of the studies explore batch reactors using low reagent concentrations. It has been shown that the experiments in a PBR improve the process metrics in relation to the results achieved in a batch reactor (BSTR) in terms of productivity and biocatalyst stability. We have found that the deactivation of the enzyme was caused by the combined effects of high temperature and initial equimolar alcohol/acid concentration ratio; the effect being stronger when acetic acid was used instead of propanoic acid. In the PBR, a loss of enzyme activity was observed at approximately 80 °C for pentyl propanoate with an alcohol/acid concentration ratio of 1, indicating that the PBR configuration increases the stability of the immobilized enzyme. The combination of the Bi−Bi Ping−Pong kinetic model and the axial dispersion flow model provides an acceptable description of the experimental behavior observed in both reactors, except under conditions where the enzymatic activity in the BSTR is notably lower than that in the PBR. We consider this work an advance in knowledge for achieving improved esterification processes in terms of sustainability and performance. It is an alternative to others proved by us[47] that have yield interesting results. In future works, economic indicators will be included to assess the purification of products resulting from the reactive operation.

APPENDIX

Appendix A RTD Data Processing

The RTD function, $E(\theta)$, and the corresponding cumulative function, $F(\theta)$, were obtained from experimental data of the pulse tracer concentration versus time θ according to the following:

$$E(\theta) = \frac{c(\theta)}{\int_0^\infty c(\theta)\mathrm{d}\theta} \qquad F(\theta) = \int_0^\theta E(\theta)\mathrm{d}\theta \tag{A.1}$$

where the integration is performed numerically. These functions, see Figure A1, were used to determine other relevant RTD moments, namely, the mean residence time, variance, and skewness,[48] expressed by

$$\theta_m = \int_0^\infty \theta E(\theta)\mathrm{d}\theta \qquad \sigma^2 = \int_0^\infty (\theta - \theta_m)^2 E(\theta)\mathrm{d}\theta$$
$$s^3 = \frac{1}{\sigma^{3/2}} \int_0^\infty (\theta - \theta_m)^3 E(\theta)\mathrm{d}\theta \tag{A.2}$$

These moments enable the calculation of the Peclet number, which is used to calculate the axial dispersion coefficient via the following equations:

$$\frac{\sigma^2}{\theta_m^2} = \frac{2}{Pe} + \frac{8}{Pe^2} \qquad D_{ax} = \frac{uL}{Pe} \tag{A.3}$$

The correlations of Kim and Kim[49] and Khaled et al.[50] are useful for calculating the porosity knowing the axial dispersion, i.e.:

$$D_{ax} = \frac{1}{20.19} d_r^{1.66} \varepsilon u d_p^{0.66} \tag{A.4}$$

The extraparticle or bed porosity is calculated directly by applying this procedure to the blue dextran RTD. The total porosity (extraparticle and intraparticle) is obtained from the sodium azide RTD as explained in Section 2.2. The intraparticle porosity is calculated by the relationship between extraparticle and total porosity; the results are shown in Table A1.

$$\varepsilon_T = \varepsilon_b + \varepsilon_p(1 - \varepsilon_b) \tag{A.5}$$

The shape of the measured RTDs indicates that the flow pattern in the packed-bed reactor is a plug-flow with a slight asymmetric axial dispersion effect, as evidenced by the calculated Peclet numbers (Pe = 24−29). Furthermore, the single clean peak shown in the RTD indicates adequate reactor packing, with no significant channeling or dead volume.[51,52] The average

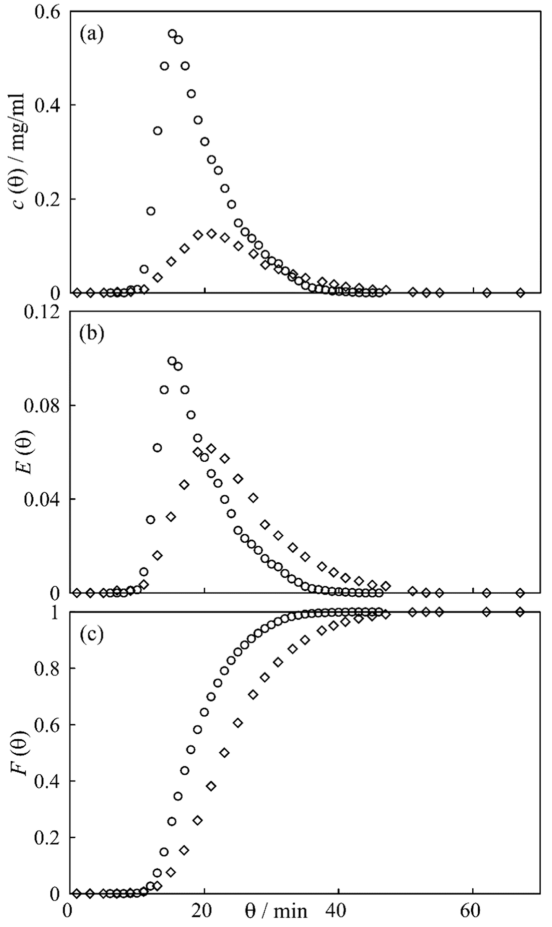

Figure A1. Experimental data of pulse tracer for (◯) blue dextran and (◇) sodium azide vs time θ for (a) concentration, (b) RTD function, $E(\theta)$, and (c) cumulative RTD function, $F(\theta)$.

Table A1. Parameters Calculated from RTD Experiments

RTD-related parameters	blue dextran	sodium azide
space−time (s−t, min)	23.46	23.46
mean residence time (θ_m, min)	19.07	24.27
variance (σ^2, min^2)	27.83	56.84
dimensionless variance (σ^2/θ_m^2)	0.0765	0.0965
skewness (s^3)	11.93	16.75
Peclet number (Pe)	29.67	24.15
axial dispersion (D_{ax}, cm^2/min)	0.282	0.346
	porosity	
total (ε_T)	0.78	
bed (ε_b)	0.64	
particle (ε_p)	0.40	

https://doi.org/10.1021/acs.iecr.5c02780
Ind. Eng. Chem. Res. XXXX, XXX, XXX−XXX

residence times show similar space-time values, see Table A1, and the calculated value of particle porosity, $\varepsilon_p = 0.4$, agrees well with other values found in the literature of $\varepsilon_p = 0.349$[53] and $\varepsilon_p = 0.5$.[54]

Appendix B Mass Transfer Calculations

B.1 External Mass Transfer. The influence of external mass transfer on the reaction rate was verified using the external effectiveness parameter η_E. For a second-order reaction in an isothermal reactor, this parameter is defined as follows:[55]

$$\eta_E = (1 - Da_{obs})^2 \quad Da_{obs} = \frac{r_{0,obs}}{k_S a c_{cat} c_0} \tag{B.1}$$

The fluid−solid mass transfer coefficient k_S shown in eq B.1 was calculated using the Sherwood number correlation for PBR reactors,[56] depending on the following dimensionless parameters:

$$Sh = \frac{k_S d_p}{D} = 1.17 Re^{0.585} Sc^{1/3}; \quad \text{being:} \quad Re = \frac{d_p u \rho}{\mu}$$
$$Sc = \frac{\mu D}{\rho} \tag{B.2}$$

The calculation of diffusivity coefficients has been described previously.[25]

B.2 Internal Mass Transfer. The influence of internal mass transfer on the overall reaction rate was checked through the internal effectiveness parameter η_I,[56] which is explicitly given by the relation:

$$\frac{r_{0,obs}}{r_0} = \eta_I = \frac{1}{\phi}\left(\frac{1}{\tanh(3\phi)} - \frac{1}{3\phi}\right) \tag{B.3}$$

where ϕ is the Thiele modulus, defined for spherical particles as

$$\phi = \frac{d_p}{6}\sqrt{\frac{r_0}{D_{eff} c_0}} \quad D_{eff} \text{ is calculated by } D_{eff} = D\frac{\varepsilon_p}{\tau} \tag{B.4}$$

According to Chowdhury et al.,[57] a tortuosity value of $\tau = 5.3$ was used.[57] The results found for the factors η_E and η_I are presented in Table B1.

The external mass transfer coefficients are very close to unity for all experiments, indicating that the transport external resistance does not affect the process rate. In contrast, the internal mass transfer affects the reaction rate in the PBR reactor, with η_I values in the range [0.85−1]. These values approach unity as the temperature increases, mainly due to the decrease in viscosity, which facilitates mass transport into the catalyst pores.

Table B1. Mass Transfer Effectiveness Factors for PBR Experiments

	external effectiveness factor, η_E		
t/°C	acetic acid, $C_{0,acoholl}/C_{0,acid} = 2$	propanoic acid, $C_{0,alcohol}/C_{0,acid} = 2$	propanoic acid, $C_{0,alcohol}/C_{0,acid} = 1$
40	0.998	0.999	0.999
50	0.999	0.999	0.999
60	0.999	0.999	0.999
70	0.999	0.999	0.999
80	0.999	0.999	0.999
	internal effectiveness factor, η_I		
t/°C	acetic acid, $C_{0,acoholl}/C_{0,acid} = 2$	propanoic acid, $C_{0,acoholl}/C_{0,acid} = 2$	propanoic acid, $C_{0,acoholl}/C_{0,acid} = 1$
40	0.869	0.852	0.893
50	0.870	0.861	0.903
60	0.893	0.869	0.943
70	0.965	0.878	0.990
80	0.995	0.884	0.998

■ ASSOCIATED CONTENT

Supporting Information

The Supporting Information is available free of charge at https://pubs.acs.org/doi/10.1021/acs.iecr.5c02780.

(Tables S1−S3) show, respectively, the properties of pure compounds, the working experimental conditions established, and the parametrization results obtained for the Bi−Bi-Ping−Pong. (Figure S1), shows the temperature effect on the conversion grade in PBR. (Figure S2) stability operation of the PBR. (Figures S3 and S4) show the effects of temperature and biocatalyst concentration on the reaction kinetic in BSTR. (Figures S5 and S6) show the operating window for BSTR and PBR (PDF)

■ AUTHOR INFORMATION

Corresponding Authors

Beatriz Lorenzo − *Division of Thermal Engineering & Instrumentation (IDeTIC), University of Las Palmas de Gran Canaria, 35017 Las Palmas de Gran Canaria, Spain;* orcid.org/0000-0003-1154-2633; Email: beatriz.lorenzo@ulpgc.es

Juan Ortega − *Division of Thermal Engineering & Instrumentation (IDeTIC), University of Las Palmas de Gran Canaria, 35017 Las Palmas de Gran Canaria, Spain;* orcid.org/0000-0002-8304-2171; Email: juan.ortega@ulpgc.es

Authors

ÁlvaroGonzález Garcinuño − *Department of Chemical Engineering, University of Salamanca, 37008 Salamanca, Spain; Institute for Biomedical Research in Salamanca (IBSAL), 37007 Salamanca, Spain;* orcid.org/0000-0003-0013-9953

EvaMartín-del Valle − *Department of Chemical Engineering, University of Salamanca, 37008 Salamanca, Spain; Institute for Biomedical Research in Salamanca (IBSAL), 37007 Salamanca, Spain;* orcid.org/0000-0003-3506-2546

Complete contact information is available at: https://pubs.acs.org/10.1021/acs.iecr.5c02780

Notes

The authors declare no competing financial interest.

■ ACKNOWLEDGMENTS

The authors are grateful for financial support from the Spanish Ministry of Science and Innovation through project PID2021-127970OB-I00. B.L. also thanks this entity for the predoctoral contract PRE2019-087401. We would like to express our gratitude to Novonesis for providing the Lypozime 435 biocatalyst utilized in the work.

■ ABBREVIATIONS

a, catalyst-specific surface area
C, concentration
C_0, initial concentration of acid or alcohol
d, diameter
Da, dimensionless Damköhler number

https://doi.org/10.1021/acs.iecr.5c02780
Ind. Eng. Chem. Res. XXXX, XXX, XXX−XXX

D, diffusivity coefficient
D_{eff}, internal effective diffusivity coefficient
D_{ax}, axial dispersion
$E(\theta)$, RTD function
$F(\theta)$, cumulative RTD function
g, gram
k_S, fluid−solid mass transfer coefficient
L, PBR length
n_D, refractive index
Pe, Peclet number
$\dot{Q}$, liquid volumetric flow
r, reaction rate
Re, Reynolds number
Sc, Schmidt number
Sh, Sherwood number
s^3, skewness
t, Celsius temperature, °C
T, temperature K
u, fluid velocity
w, weight
z, longitudinal distance
ε, porosity
ε_p, enzyme porosity
ε_b, bed porosity
ϕ, Thiele's module
η_E, external mass transfer effectiveness coefficient
η_I, internal mass transfer effectiveness coefficient
μ, viscosity
θ, residence time
θ_m, mean residence time
ρ, density
σ^2, variance
τ, tortuosity
BET, Brunauer−Emmett−Teller method
BSTR, Batch stirred tank reactor
PLU, propylene laurate units specific unit of measurement for lipase activity
PBR, packed-bed-reactor
PSD, particle size distribution
RTD, residence time distribution

REFERENCES

(1) Tufvesson, T.; Lima-Ramos, J.; Haque, N. A.; Gernaey, K. V.; Woodley, J. M. Advances in the process development of biocatalytic processes. *Org. Process Res. Dev.* **2013**, *17*, 1233−1238.

(2) Meissner, M. P.; Woodley, J. M. Mass-based biocatalyst metrics to guide protein engineering and bioprocess development. *Nat. Catal.* **2022**, *5*, 2−4.

(3) Salvi, H. M.; Yadav, G. D. Process intensification using immobilized enzymes for the development of white biotechnology. *Catal. Sci. Technol.* **2021**, *11*, 1994−2020.

(4) Sousa, R. R.; Silva, A. S. A.; Fernandez-Lafuente, R.; Ferreira-Leitão, V. S. Solvent-free esterifications mediated by immobilized lipases: a review from thermodynamic and kinetic perspectives. *Catal. Sci. Technol.* **2021**, *11*, 5696−5711.

(5) Basso, A.; Serban, S. Industrial applications of immobilized enzymes—A review. *J. Mol. Catal.* **2019**, *479*, 110607−110626.

(6) DiCosimo, R.; McAuliffe, J.; Poulose, A. J.; Bohlmann, G. Industrial use of immobilized enzymes. *Chem. Soc. Rev.* **2013**, *42*, 6437−6474.

(7) Wang, L.; Chen, G.; Tang, J.; Ming, M.; Jia, C.; Feng, B. Continuous biosynthesis of geranyl butyrate in a circulating fluidized bed reactor. *Food Biosci.* **2019**, *27*, 60−65.

(8) Chang, S.-W.; Shaw, J.-F.; Yang, C.-K.; Shieh, C.-J. Optimal continuous biosynthesis of hexyl laurate by a packed bed bioreactor. *Process Biochem.* **2007**, *42*, 1362−1366.

(9) Salvi, H. M.; Kamble, M. P.; Yadav, G. D. Synthesis of Geraniol Esters in a Continuous-Flow Packed-Bed Reactor of Immobilized Lipase: Optimization of Process Parameters and Kinetic Modeling. *Appl. Biochem. Biotechnol.* **2018**, *184*, 630−643.

(10) Damnjanović, J. J.; Žuža, M. G.; Savanović, J. K.; Bezbradica, D. I.; Mijin, D. Ž.; Bošković-Vragolović, N.; Knežević-Jugović, Z. D. Covalently immobilized lipase catalyzing high-yielding optimized geranyl butyrate synthesis in a batch and fluidized bed reactor. *J. Mol. Catal. B: Enzym.* **2012**, *75*, 50−59.

(11) Bhavsar, K. V.; Yadav, G. D. n-Butyl levulinate synthesis using lipase catalysis: comparison of batch reactor versus continuous flow packed bed tubular microreactor. *J. Flow Chem.* **2018**, *8*, 97−105.

(12) Matte, C. R.; Bordinhaõ, C.; Poppe, J. K.; Rodrigues, R. C.; Hertz, P. F.; Ayub, M. A. Z. Synthesis of butyl butyrate in batch and continuous enzymatic reactors using Thermomyces lanuginosus lipase immobilized in Immobead 150. *J. Mol. Catal. B: Enzym.* **2016**, *127*, 67−75.

(13) Vilas Bôas, R. N.; Ceron, A. A.; Bento, H. B. S.; de Castro, H. F. Application of an immobilized Rhizopus oryzae lipase to batch and continuous ester synthesis with a mixture of a lauric acid and fusel oil. *Biomass Bioenergy* **2018**, *119*, 61−68.

(14) Carta, G.; Gainer, J. L.; Gibson, M. E. Synthesis of esters using a nylon-immobilized lipase in batch and continuous reactors. *Enzyme Microb. Technol.* **1992**, *14*, 904−910.

(15) Mensah, P.; Gainer, J. L.; Carta, G. Adsorptive Control of Water in Esterification with Immobilized Enzymes: II. Fixed-Bed Reactor Behavior. *Biotechnol. Bioeng.* **1998**, *60*, 445−453.

(16) Mensah, P.; Carta, G. Adsorptive Control of Water in Esterification with Immobilized Enzymes. Continuous Operation in a Periodic Counter-Current Reactor. *Biotechnol. Bioeng.* **1999**, *66*, 137−146.

(17) Skoronski, E.; Padoin, N.; Soares, C.; Furigo, A. Stability of immobilized Rhizomucor miehei lipase for the synthesis of pentyl octanoate in a continuous packed bed bioreactor. *Braz. J. Chem. Eng.* **2014**, *31*, 633−641.

(18) Vasilescu, C.; Paul, C.; Marc, S.; Hulka, I.; Péter, F. Development of a Tailored Sol-Gel Immobilized Biocatalyst for Sustainable Synthesis of the Food Aroma Ester n-Amyl Caproate in Continuous Solventless System. *Foods* **2022**, *11*, 2485.

(19) Calinescu, I.; Vartolomei, A.; Gavrila, I.-A.; Vinatoru, M.; Mason, T. J. A reactor designed for the ultrasonic stimulation of enzymatic esterification. *Ultrason. Sonochem.* **2019**, *54*, 32−38.

(20) Pires-Cabral, P.; da Fonseca, M. M. R.; Ferreira-Dias, S. Esterification activity and operational stability of Candida rugosa lipase immobilized in polyurethane foams in the production of ethyl butyrate. *Biochem. Eng. J.* **2010**, *48*, 246−252.

(21) Romero, M. D.; Calvo, L.; Alba, C.; Habulin, M.; Primožič, M.; Knez, Z. Enzymatic synthesis of isoamyl acetate with immobilized Candida antarctica lipase in supercritical carbon dioxide. *J. Supercrit. Fluids* **2005**, *33*, 77−84.

(22) Gillies, B.; Yamazaki, H.; Armstrong, D. W. Production of flavor esters by immobilized lipase. *Biotechnol. Lett.* **1987**, *9*, 709−714.

(23) Pierotti, G. J.; Wilson, R. A.; Anderson, E. A. Purification of penicillin, U.S. Patent 2,503,216 A. 1946.

(24) Souders, M., Jr. Penicillin extraction process, U.S. Patent 2,488,559 A. 1948.

(25) Lorenzo, B.; Fernández, L.; Ortega, J.; Domínguez, L. Improvements in the Modeling and Kinetics Processes of the Enzymatic Synthesis of Pentyl Acetate. *Processes* **2023**, *11*, 1640.

(26) Riddick, J. A.; Bunger, W. B.; Sakano, T. K. *Organic Solvents: Physical Properties and Methods of Purification*; Wiley-Interscience: New York, 1986.

(27) Ortega, J.; Matos, J. S. Estimation of the isobaric expansivities from several equations of molar refraction for some pure organic compounds. *Mater. Chem. Phys.* **1986**, *15*, 415−425.

https://doi.org/10.1021/acs.iecr.5c02780
Ind. Eng. Chem. Res. XXXX, XXX, XXX−XXX

(28) Granados, K.; Gracia-Fadrique, J.; Amigo, A.; Bravo, R. Refractive Index, Surface Tension, and Density of Aqueous Mixtures of Carboxylic Acids at 298.15 K. *J. Chem. Eng. Data* **2006**, *51*, 1356−1360.
(29) TRC *Thermodynamic Tables Non-Hydrocarbons*; Thermodynamic Research Center; Texas A&M University System: College Station, TX, 1993; . Extant 2013.
(30) dos Santos, P.; Zabot, G. L.; Meireles, M. A. A.; Mazutti, M. A.; Martínez, J. Synthesis of eugenyl acetate by enzymatic reactions in supercritical carbon dioxide. *Biochem. Eng. J.* **2016**, *114*, 1−9.
(31) Baião Dias, A. L.; da Cunha, G. N.; dos Santos, P.; Meireles, M. A. A.; Martínez, J. Fusel oil: Water adsorption and enzymatic synthesis of acetate esters in supercritical CO2. *J. Supercrit. Fluids* **2018**, *142*, 22−31.
(32) Rodrigues, A. E. Residence time distribution (RTD) revisited. *Chem. Eng. Sci.* **2021**, *230*, 116188.
(33) Viet, D.; Beck-Candenedo, E.; Gray, D. G. Synthesis and characterization of blue dextrans. *Carbohydr. Polym.* **2008**, *74* (3), 372−378.
(34) Gustavsson, P.-E.; Larsson, P.-O. Continuous superporous agarose beds in radial flow columns. *J. Chromatogr. A* **2001**, *925*, 69−78.
(35) Aguiar, L. G.; Godoy, W. M.; Graça, N. A. B. S.; Rodriguez, A. L. Resin-catalyzed reaction modeling integrating catalyst swelling and sites accessibility: Application to solketal synthesis. *Chem. Eng. Res. Des.* **2024**, *212*, 58−70.
(36) Xu, L.; Wang, J.; Huang, F.; Zheng, M. An efficient and robust continuous-flow bioreactor for the enzymatic preparation of phytosterol esters based on hollow lipase microarray. *Food Chem.* **2022**, *372*, 131256.
(37) Kuo, C.-H.; Huang, C.-Y.; Lee, C.-L.; Kuo, W.-C.; Hsieh, S.-L.-; Shieh, C.-J. Synthesis of DHA/EPA Ethyl Esters via Lipase-Catalyzed Acidolysis Using Novozym® 435 A Kinetic Study. *Catalysts* **2020**, *10*, 565.
(38) Xiao, Y.; Zheng, M.; Greek lettersZ, L.; Shi, J.; Huang, F.; Luo, X. Constructing a Continuous Flow Bioreactor Based on a Hierarchically Porous Cellulose Monolith for Ultrafast and Nonstop Enzymatic Esterification/Transesterification. *ACS Sustain. Chem. Eng.* **2019**, *7*, 2056−2063.
(39) Wang, J.; Gu, S.-S.; Cui, H.-S.; Yang, L.-Q.; Wu, X.-Y. Rapid synthesis of propyl caffeate in ionic liquid using a packed bed enzyme microreactor under continuous-flow conditions. *Bioresour. Technol.* **2013**, *149*, 367−374.
(40) Stempfer, G.; Höll-Neugebauer, B.; Kopetzki, E.; et al. A fusion protein designed for noncovalent immobilization: stability, enzymatic activity, and use in an enzyme reactor. *Nat. Biotechnol.* **1996**, *14*, 481−484.
(41) Maria, G. Enzymatic reactor selection and derivation of the optimal operation policy, by using a model-based modular simulation platform. *Comput. Chem. Eng.* **2012**, *36*, 325−341.
(42) Denčić, I.; de Vaan, S.; Noël, T.; Meuldijk, J.; de Croon, M.; Hessel, V. Lipase-based biocatalytic flow process in a packed-bed microreactor. *Ind. Eng. Chem. Res.* **2013**, *52*, 10951−10960.
(43) Gao, Y.; Muzzio, F. J.; Ierapetritou, M. G. A review of the Residence Time Distribution (RTD) applications in solid unit operations. *Powder Technol.* **2012**, *228*, 416−423.
(44) Chung, S. F.; Wen, C. Y. Longitudinal dispersion of liquid flowing through fixed and fluidized beds. *AIChE J.* **1968**, *14*, 857−866.
(45) Danckwerts, P. V. Significance of Liquid-Film Coefficients in Gas Absorption. *Ind. Eng. Chem.* **1951**, *43*, 1460−1467.
(46) Kierzenka, J.; Shampine, L. F. A BVP solver based on residual control and the Maltab PSE. *ACM Trans. Math Software* **2001**, *27*, 299−316.
(47) Lorenzo, B.; Granca, N. S.; Ortega, J.; Rodrigues, A. E. Operation and Modeling of a Process for 1,1-Diethoxybutane Synthesis in a Simulated Moving Bed Reactor Pilot Unit. *Ind. Eng. Chem. Res.* **2024**, *63*, 21190−21199.
(48) Fogler, H. S. *Elements of Chemical Reaction Engineering*, 4 ed.; Prentice Hall PTR, 2006.
(49) Kim, S. D.; Kim, C. H. Axial dispersion characteristics of three phase fluidized beds. *J. Chem. Eng. Jpn.* **1983**, *16*, 172−178.
(50) Khaled, G.; Bourouina-Bacha, S.; Sabiri, N.-E.; Tighzert, H.; Kechroud, N.; Bourouina, M. Simplified correlations of axial dispersion coefficient and porosity in a solid-liquid fluidized bed adsorber. *Exp. Therm. Fluid Sci.* **2017**, *88*, 317−325.
(51) Sánchez, A.; Valero, F.; Lafuente, J.; Solà, C. Highly enantioselective esterification of racemic ibuprofen in a packed bed reactor using immobilised Rhizomucor miehei lipase. *Enzyme Microb. Technol.* **2000**, *27*, 157−166.
(52) Franklin, R. D.; Whitley, J. A.; Caparco, A. A.; Bommarius, B. R.; Champion, J. A.; Bommarius, A. S. Continuous production of a chiral amine in a packed bed reactor with co-immobilized amine dehydrogenase and formate dehydrogenase. *Chem. Eng. J.* **2021**, *407*, 127065.
(53) Haigh, K. F.; Abidin, S. Z.; Vladisavljević, G. T.; Saha, B. Comparison of Novozyme 435 and Purolite D5081 as heterogeneous catalysts for the pretreatment of used cooking oil for biodiesel production. *Fuel* **2013**, *111*, 186−193.
(54) Dong, H.-P.; Wang, Y.-J.; Zheng, Y.-G. Enantioselective hydrolysis of diethyl 3-hydroxyglutarate to ethyl (S)-3-hydroxyglutarate by immobilized Candida antarctica lipase B. *J. Mol. Catal. B: Enzym.* **2010**, *66*, 90−94.
(55) Carberry, J. *Chemical and Catalytic Reaction Engineering*; Dover Publications: New York, 2001.
(56) Smith, J. *Chemical Engineering Kinetics*, 3 ed.; McGraw Hill, 1981.
(57) Chowdhury, A.; Mitra, D. A kinetic study on the Novozyme 435-catalyzed esterification of free fatty acids with octanol to produce octyl esters. *Biotechnol. Prog.* **2015**, *31*, 1494−1499.

https://doi.org/10.1021/acs.iecr.5c02780
Ind. Eng. Chem. Res. XXXX, XXX, XXX−XXX